Formation of Hybrid Resonators in the Semiconductor Circular Ring Laser Diode and Its Output Characteristics

Chun Ting Tsen, Ming Chang Shih and Wen Ho Lan
Department of Electrical Engineering, National University of Kaohsiung, Kaohsiung, R.O.C., Taiwan

Keywords: Semiconductor Laser Diode, Circular Ring Resonator, Optical Nonlinearity, Conjugate Reflection.

Abstract: We present the study of the emission characteristics of a semiconductor circular ring laser diode with a Y-junction output coupler. Instead of laser output from Y-junction coupling terminal, a confined laser beam output was also observed at non-waveguide region due to optical nonlinearity effect of the multi-quantum wells active median. It showed that except for the circular ring resonator mode, much complicate modes were excited from both output terminals. A hybrid resonator formed by conjugated reflection is suggested to explain the features of output characteristics. In addition, L-I and spectrum characteristics of both output terminals of these hybrid resonators were analysed to explore the detailed mechanism of these hybrid resonator.

1 INTRODUCTION

Semiconductor laser diode with circular ring resonator SCRLD had been attracted interest of research for its long optical path way advantage of strong side modes rejection and flexibility to be integrated with other passive components for the development of more advanced opto-electronic systems. Recently, it was demonstrated the control of CW/CCW mode of the SCRLD output by external injection light that makes it an ideal all light wave signal processing system. There are also applications of SCRLD to achieve wavelength filtering and tuning of the laser output. However, there is not many studies about the nonlinearity effect of the SCRLD. We have studied these devices for decades to show that instead of linear operation laser mechanism, it is possible to excited more complex optical nonlinear effects in these SCRLD devices due to strong nonlinear coefficient of these multi-quantum wells active material. We had demonstrated the generation of Soliton waveguide in a SRCLD with a Y- junction output coupler and switching control of light beam coupling. Here we present the study of the formation of hybrid resonator due to phase conjugate reflection in this SCRLD device and its output characteristics.

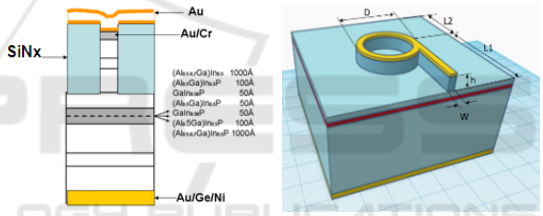

Figure 1: Material structure and dimensions of the fabricated SRCLD.

2 FABRICATION OF THE SCRLD DEVICE

As shown in Fig.1, the fabricated SCRLD was fabricated with a metal organic chemical vaper deposition (MOCVD) grown GaInP/InGaAlP multiple-quantum-well(MQW) active structure with gain spectrum around 650 nm. Figure 2 shows the device process flow. First, a SiO_2/Au/Cr layer with the device pattern was achieved by a lift-off process. Then, structure of the circular ring resonator with diameter D = 500 μm ~1000 μm , depth h= 0.85 μm ~0.9 μm , width W=10 μm ~25 μm , and the Y-junction coupling section was etched by inductively coupled plasma (ICP) etching.

Tsen, C., Shih, M. and Lan, W.
Formation of Hybrid Resonators in the Semiconductor Circular Ring Laser Diode and Its Output Characteristics.
DOI: 10.5220/0010391301310135
In *Proceedings of the 9th International Conference on Photonics, Optics and Laser Technology (PHOTOPTICS 2021)*, pages 131-135
ISBN: 978-989-758-492-3

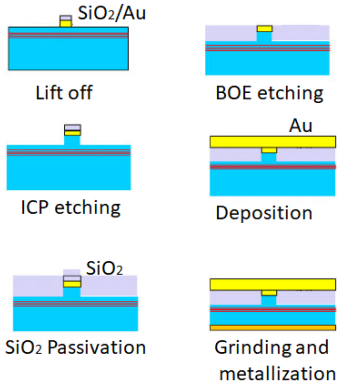

Figure 2: Device process flow of the SCRLD.

To eliminate the problem of short contact between the p-n junction, the depth of the ridge waveguide was etched about 0.8 µm located at just a distances above the active layer. Secondly, a passivation layer of the SiO_2 thin film was deposited using sputtering. Then, an etch back process was applied to etch out the SiO_2 layer by using BOE wet etching to open the electrode area. Then, a blank layer of Au (200 nm)/Cr (10 nm) was deposited on the SiO_2 passivation layer. Then, the substrate was grinded down to a thickness of 150 µm to minimize the resistivity through the substrate. Finally, an AuGe/Ni alloy thin film was deposited on the back side for n-type metal contact and then by annealing the device at 650 °C for 30 s. The fabricated device was cleaved by a diamond scriber and tested on a micro probing station.

3 OUTPUT CHARCTERIZATIONS

The fabricated SCRLD device was probe-tested on a micro-probing station for light-current (L-I) and spectrum measurements. Fig. 2 shows the schematics of the output characterization system in which an HP 8114A pulse power source was operating at 1 kHz for the current injection on the test device. By using a beam splitter cube, the output emission can be measured by the Si-based photodetector for L-I characterization, and the Jobin Yvon SPEX 500 spectrometer with resolution of 0.01 nm to analyse the spectrum of the output emission in the same time. All devices are connected with a PC by GPIB interfacing for control and data processing. The output emission from the tested device was collimated by an object lens (x10) then through a beam splitter by which to guide part of the emission to an IR CCD for visualization of the side view of the emission from the SCRLD.

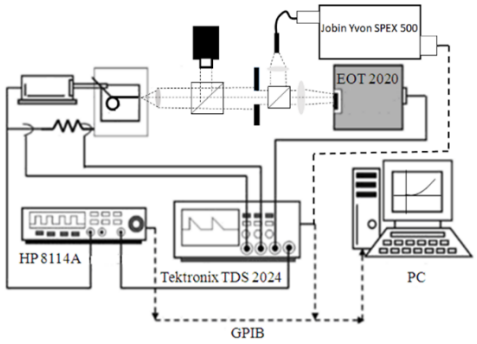

Figure 3: Schematics of the output characterization system.

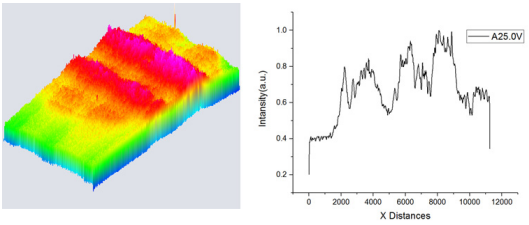

Figure 4: CCD image and profile of the emission from terminal "S", which shows high order soliton characteristic.

Instead of strong laser emission observed from the Y-junction ridge waveguide output coupling terminal (marked as "Y"), it was also observed a strong and confined emission at the opposite direction of terminal Y on non-waveguide region(marked as "S"). Fig. 4 shows the far field CCD image and profile of the emission from terminal "S", which shows high order soliton characteristic.

We had previously reported that the confined emission from the non-waveguide region was the formation of spatial soliton due to the strong 3rd order nonlinearity of the multiple quantum wells medium. In principle, the spatial solitons formed as the normal diffraction of the medium can be exactly balanced by refractive index changes induced by the electro-optic nonlinear effect. Since the Kerr effect constant of most of the optical materials is relatively small, a power density of light on the order of MW/cm^2 is required to form Kerr effect solitons. It was reported that spatial solitons could be excited by electric-field-induced refraction index changes in photorefractive or photovoltaic media. In the case of photorefractive spatial solitons, the distribution of the field intensity of a light beam modulates the index of refraction of the medium via the photorefractive effect, which compensates for the natural diffraction and achieves the confinement of the beam profile along the propagation direction. Photorefractive spatial solitons can be formed at a relatively lower power of around 100mW that makes them attractive for applications in

integrated optoelectronic devices such as all-optical light wave control of guiding, switching, and signal modulation.

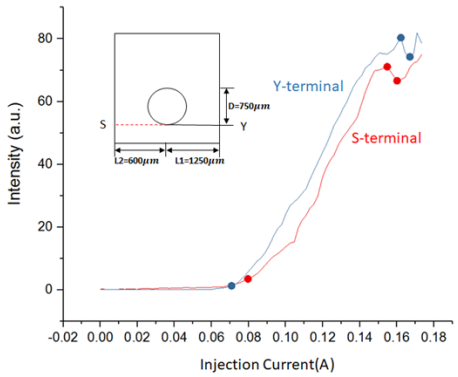

Figure 5: L-I measurement of the SRCLD with diameter D= 750 um, the length of Y-junction coupling section L_1=1250 um, and the length of non-waveguide section L_2=600 um.

Fig. 5 shows the L-I measurements at both terminal "Y" and terminal "S" of a SCRLD with D=750 μm , W= 20 μm , h= 0.9 μm , length of Y-junction coupling section L_1=1250 μm , and length of soliton resonator L_2=600 μm . Threshold currents of both outputs terminal are very close at 0.06 A(~60 A/cm^2). Fig. 7a shows the emission spectrum from Y-junction terminal "Y" with various injection bias. The emission peak at 652.80 nm is referred to the CW and CCW propagation mode in the circular ring resonator and being coupled out through the Y-junction coupler. As the injection current increase; from 0.1 A to 0.14 A, new spectral peaks located at 650.0 nm and 656.0 nm starting to take off. Peaks position of λ_1=652.8 nm, λ_2=650.0 nm, and λ_3=656.0 nm are very close to the relationship of four waves mixing as

$$\frac{2}{\lambda_1} = \frac{1}{\lambda_2} + \frac{1}{\lambda_3}$$

due to 3rd order optical nonlinearity excited by CW/CCW propagation modes in the circular ring resonator. It is worth to note that λ_1=652.8 nm might referred as the zero dispersion point for this four wave mixing; FWMX system. Fig. 7b shows the emission spectrum at soliton terminal "S" that seems close to the spectrum of terminal "Y" only with a little deviations of the position between these two spectrums. In addition to the spectrum measurements, a polarizer was place at the entrance of the Jobin Yvon SPEX 500 spectrometer to examine the polarization of the emission. The result showed that the emissions from both hybrid resonators were linear polarized as expected. Fig. 6 shows the measurement of the polarization scan of the emission from soliton output terminal.

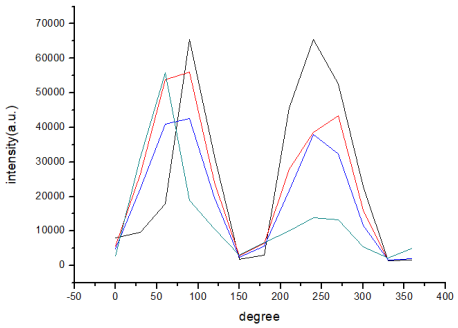

Figure 6: Polarization scan of the emission from the soliton output terminal.

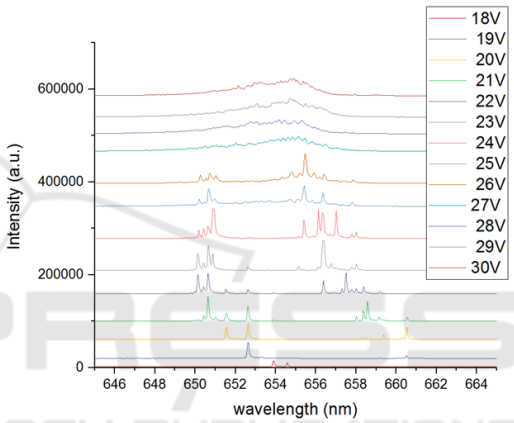

Figure 7a: Emission spectrum from the Y-junction resonator.

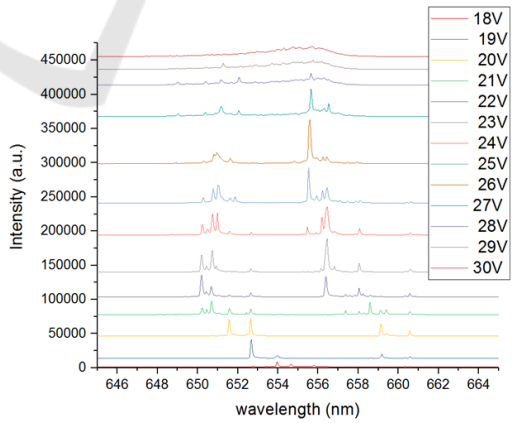

Figure 7b: Emission spectrum from the soliton resonator.

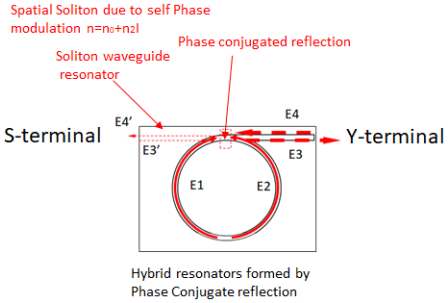

Figure 8: Schematic diagram that described the formation of the hybrid resonator.

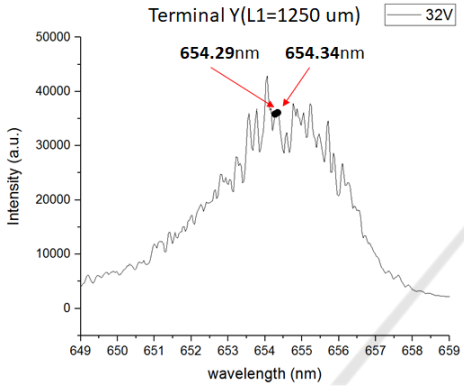

Figure 9a: Emission spectrum at high current injection from the Y-junction resonator with resonator length L_1=1250 um.

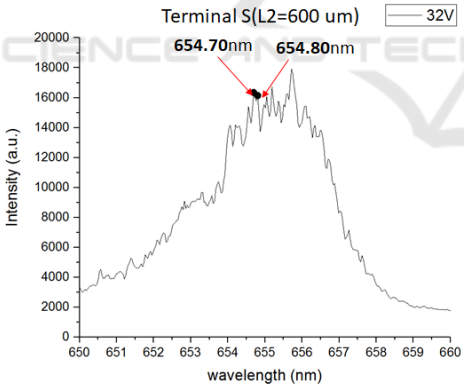

Figure 9b: Emission spectrum at high current injection from the soliton resonator of a length L_2=600 um.

At high injection up to 0.16 A, it is shown that discrete peaks λ_2=650.0 nm and λ_3=656.0 are diminishing by taking off a broaden multi-modes spectrum features located at 654 nm.

A model of hybrid resonator formation is described in Fig. 8. In the MWQ material with high 3rd order nonlinearity coefficient, phase conjugate reflection can be excited at the intersection region of the Y-junction coupling section and the circular ring resonator by counter propagating modes of E_1(CW) and E_2(CCW) in the ring resonator. Light reflected from the cleaved mirror at the end of the ridge waveguide Y-junction coupling terminal will be amplified by phase conjugated reflection and form a linear resonator. By the same way, another linear resonator located at the opposite direction of the Y-junction coupling section can also be formed due to the confinement of the spatial soliton and amplification by conjugated reflection. The light amplification factor is increasing with the intensity of the ring resonator. In fact, lasing condition of this case is required by the longitudinal modes of the linear resonator and the FWMX phase matching condition.

It is explained that spectrum peaks of λ_2=650.0 nm and λ_3=656.0 are dominating in the emission of the hybrid resonator. As the injection current keep increasing to the oscillating point of the conjugate reflection, the amplification factor of the resonator drops, as a result the loss of the linear resonator increase and the emission become broaden. In Fig.5, a turning point at 0.16 A of the L-I curve is referred to the reaching of the oscillating point of the conjugate reflection.

In principle, the circular ring resonator function as the pumping source for the generation of optical nonlinearity effect and the outputs modes of the hybrid resonator are controlled by the optical property of itself. Fig. 9a shows the detailed spectrum of the longitudinal modes of the Y-junction resonator of a length L_1=1250 μm at current injection above 0.16A. The modes spacing of 0.05 nm is close to the calculated value using parameter of index of reflection n=3.6 of the laser medium and the resonator length of L_1=1250 μm . Fig.9b shows the emission spectrum of the soliton resonator of a length L_2=600 μm . It shows that the modes spacing of 0.1 nm which is also very close to calculated value using the resonator length of L_2=600 μm .

4 CONCLUSIONS

We have demonstrated that the formation of hybrid resonators of the SCRLD and its output characteristics. The conjugated reflection excited by the strong emission in the circular ring resonator play an important role to the formation of hybrid resonators. Since the FWMX is coherent light interaction in nature thus suggested the laser emission from the hybrid resonator is coherent, and it is essential for the development of more advanced opto-electronic devices applying coherent signal

processing. Further experimental results to explore the nonlinearity effect in the SCRLD will be presented in the near future.

ACKNOWLEDGEMENTS

We would like to thank to Union Optronics Corporation for their help in device processing and Ms. W. C. Lin and colleagues for preparing the experimental data and manuscript. We would also like to thank the Ministry of Sciences and Technology in Taiwan for funding this research under the project number of 107-2221-E-390-014.

REFERENCES

D. S. Chemla, D. A. B. Miller, and P. W. Smith, 1985, Optical Engineering 24(4), 556 -564.

B. Li, D. Lu, M.I. Memon, G. Mezosi, Z.Wang, M. Sorel and S. Yu ,2009, Electronics Letters, Vol. 45 No. 13.

Julien Javaloyes, and Salvador Balle, 2011, IEEE Journal of Quantum Electronics, VOL. 47, NO. 8, AUGUST.

Sorel, M, Laybourn, PJR, Giuliani, G, and Donati, S, 2002, Applied Physics Letters, 80 . pp. 3051-3053.

Mezosi, G., Strain, M. J. , Furst, S., Wang, Z., Yu, S., and Sorel, M. , 2009, IEEE Photonics Technology Letters, 21 (2). pp. 88-90.

Thakulsukanant, K., Li, B., Memon, I., Mezosi, G. , Wang, Z. R., Sorel, M. , and Yu, S. Y., 2009, Journal of Lightwave Technology, 27 (6). pp. 631-638.

Carsten Thirstrup, Peter N. Robson, Patrick Li Kam Wa, Malcolm A. Pate, C. C. Button, and J. *S*. Roberts, 1992, IEEE Journal of Quantum Electronics, VOL. 28, NO. 4.

M.C. Shih, S. C. Wang, C. E. Ho, 2009, Japanese Journal of Applied Physics. 48.

M. C. Shih and C. S. Chen, 2011, Japanese Journal of Applied Physics. 50.

G. A. Swartzlander, D. R. Anderson, J. J. Regan, H. Yin, and A. E. Kaplan, 1991, Phys. Rev. Lett. 66, 1583.

J. S. Aitchison, A. M. Weiner, Y. Silberberg, M. K. Oliver, J. L. Jackel,D. E. Leaird, E. M. Vogel, and P. W. E. Smith, 1990, Opt. Lett. 15, 471.

M. D. Iturbe Castillo, J. J. Sanchez-Mondragon, and S. Stepanov, Opt. Lett.21, 1622 (1996).

M. Segev, 1998, Opt. Quantum Electron. 30, 503.

X. Hutsebaut, C. Cambournac, M. Haelterman, J. Beeckman, and K. Neyts, 2005, J. Opt. Soc. Am. B 22, 1424.

C. Conti, M. Peccianti, and G. Assanto, 2004, Phys. Rev. Lett. 92, 113902.

G. I. Stegeman and M. Segev, 1999, Science 286, 1518.

M. Peccianti, A. Dyadyusha, M. Kaczmarek, and G. Assanto, 2008, Phys. Rev. Lett. 101, 153902.

C. P. Jisha, A. Alberucci, R. K. Lee, and G. Assanto, 2013, Opt. Express 21,18646.